Fifth Asian Conference on Computer Visio, January 2002

Trail-Dependent Intelligent Scissors Based on Multi-Scale Image Segmentation

Yi-Ping Hung and Yu-Pao Tsai
Institute of Information Science, Academia Sinica, Taipei, Taiwan, R.O.C.

Abstract

Image segmentation is a very important topic in computer vision. However, due to the large variation of image content, fully automatic image segmentation for general applications is still an open problem. Therefore, our goal is to develop an interactive image segmentation tool that can accurately extract the desired object boundaries with minimal human efforts. In this paper, we propose a new trail-dependent intelligent scissors, which let the user interactively extract desired object boundaries based on multi-scale image segmentation. By utilizing the information contained in the trail of the cursor's motion, which somewhat implies the intention of the human operator, our intelligent scissors can allow the user to extract a desired object boundary with less mouse-clicking, and hence is more user-friendly. This is the major advantage of our new intelligent scissors. Another advantage is that our intelligent scissors permits the user to trace the object boundary with less tension by utilizing the coarse-to-fine region boundaries provided by multi-scale image segmentation. Our experiments have demonstrated that the new interactive segmentation tool requires less human efforts than the previously available tools.

1. Introduction

Image segmentation is a very important topic in computer vision. However, due to the large variation of image content, fully automatic image segmentation for general applications is still an open problem. Therefore, our goal is to develop an interactive image segmentation tool that can accurately extract the desired object boundary with minimal human efforts.

Typical examples of interactive image segmentation tools are magic wand, active contour [2] [5**]** [14] and intelligent scissors [6] [7]. Magic wand is a segmentation tool that can be found in Photoshop. When a user selects a sample pixel with the magic wand, a connected region will be formed, which consists of all the pixels that fall within an adjustable tolerance of the sample pixel. Active contour is another common tool for image segmentation. It starts with a given initial contour around the desired object, and seeks a better contour encompassing the desired object by minimizing an energy functional that combines internal forces, such as gradient magnitude, with external forces, such as boundary curvature. Intelligent scissors interactively shows the optimal path, which is supposed to coincide with the desired object boundary, from a given seed point to the current cursor position. Among the above three tools, intelligent scissors is probably the most intuitive one to use since the user can trace the desired boundary by interactively modify the cursor point, while it is harder to predict the extracted boundary produced by the magic wand or active contour algorithm.

To speed up the optimal path computation in the above-mentioned “pixel-based” intelligent scissors, Mortensen and Barrett recently proposed a region-based intelligent scissors based on toboggan image segmentation [8]. A brief review on intelligent scissors will be given in Section 2. Although the intelligent scissors is relatively intuitive to use, there is still much room for improvements. A problem with the previous intelligent scissors is that the boundaries extracted are trail-independent. That is, the extracted boundary depends only on the image positions of the seed point and the current cursor point, and is not dependent on how the human operator moves the cursor from the seed point to the current cursor point.

In this paper, we propose a new trail-dependent intelligent scissors, which let the user interactively extract desired object boundaries based on multi-scale watershed image segmentation. By utilizing the information contained in the trail of the cursor’s motion, which somewhat implies the intention of the human operator, our intelligent scissors can allow the user to extract a desired object boundary with less mouse-clicking, and hence is more user-friendly. This is the major advantage of our new intelligent scissors. Another advantage is that our intelligent scissors permits the user to trace the object boundary with less tension by utilizing the coarse-to-fine region boundaries provided by multi-scale watershed segmentation. More specifically, by choosing a coarser scale in watershed segmentation, the user no longer have to carefully move the cursor in order to follow the desired boundary very precisely (please refer to example given in Section 3.1 and Figure 2). The drawback of using "coarser-scale" watershed segmentation is that some weaker boundaries can not be extracted by the intelligent scissors since they do not even appear as potential edges in the watershed segmentation result. Fortunately, this can be amended by manually adjusting the scale of watershed segmentation to a finer scale for that particular portion of boundaries. In summary, instead of repeating "careful clicking" when using the conventional intelligent scissors, the trail-dependent intelligent scissors usually requires only one initial "careful clicking," which is then followed by continuous "casual tracing" of the desired object boundary.

The remainder of this paper is organized as follows. Section 2 gives a brief review of the conventional intelligent scissors, and introduces some basic concepts and terminology that will be used in Section 3. Details of the proposed trail-dependent intelligent scissors are presented in Section 3. In Section 3.1, we focus on the multi-scale region-based technique. In Section 3.2, we focus on the trail-dependent technique. Section 4 shows some experimental results and demonstrates the advantages of our method. Finally, Section 5 gives a conclusion.

2. Review of Intelligent Scissors

As mentioned in the last section, intelligent scissors [6] [7] is an interactive image segmentation tool that allows the human operator to extract desired object boundaries by selecting a sequence of optimal paths corresponding to object boundaries. First, the input image is considered as a weighted graph. All pixels of the input image are nodes of the weighted graph, with weighted edges connecting each pixel with its eight adjacent neighbors.

The local cost on a weighted edge $E(p,q)$ is calculated by a cost function $Cost(p,q)$ in equation (1).

$$\begin{aligned} Cost(p,q) = w_Z \cdot f_Z(q) + w_G \cdot f_G(q) + w_D \cdot f_D(p,q) + \\ w_P \cdot f_P(q) + w_I \cdot f_I(q) + w_O \cdot f_O(q) \end{aligned} \tag{1}$$

where f_Z, f_G, f_D, f_P, f_I and f_O are the image feature function of Laplacian zero-crossing, gradient magnitude, gradient direction, edge pixel value, “inside” pixel value and “outside” pixel value, respectively. Each w is the weight of the corresponding feature function.

After the weighted graph is constructed, the human operator then selects a seed point. The optimal paths from the seed point to each pixel are determined by applying Dijkstra’s shortest path searching algorithm. Next, when the human operator moves the cursor to an image position lying on the object boundary he desires, the piece-wise optimal path between the seed point and the current cursor point will be displayed accordingly. This segment of optimal path is called a “live-wire”.

If this segment of “live-wire” coincides with the object boundary the user desires, he can then click the mouse button to select this segment of “live-wire”, and the current cursor point will become the new seed point. The above procedure of “live-wire” selection will be repeated until the contour of the desired object boundary has been completely extracted. In short, the problem of object contour extraction is solved by interactively selecting those piece-wise optimal paths.

In 1999, Mortensen and Barrett proposed a region-based intelligent scissors to speedup the pixel-based intelligent scissors. First, they partitioned the input image into a collection of regions using the toboggan algorithm. Figure 1(c) shows an example of the result obtained by applying the toboggan segmentation to the gradient image shown in Figure 1(b). Notice that the gray level of Figure 1(b) represents the gradient value of the computer-generated input image shown in Figure 1(a). The darker pixels have higher gradient value. After applying the toboggan segmentation, each connected region is assigned with a different label. In Figure 1(c), different labels are rendered with different colors. Next, a weighted graph is constructed by tracing the boundary of each region successively. The nodes of the weighted graph are created at the site where 3 or 4 regions meet at one single pixel. Each edge of the weighted graph is a segment of the region boundary that connects two nodes, as illustrated in Figure 1(c).

Notice that, after applying the toboggan algorithm, each edge of the weighted graph corresponds to a segment of region boundary that is composed of sequence of pixel "cracks" (the "crack" between two neighboring pixels). Let $L(p)$ and $N(p)$ denote the label of pixel *p* and the 4-connected neighborhood of pixel *p*, respectively. The pixel crack between *p* and *q* is defined as the ordered pair (p,q) such that $q \in N(p)$ and $L(p) \neq L(q)$, and the crack direction vector, $d_{p,q} = \begin{bmatrix} 0 & -1 \\ 1 & 0 \end{bmatrix}(p-q)$, is the vector pointing clockwise relative to *p*. Consider a region with label *l*, and suppose that its region boundary is composed of a sequence of pixel cracks, denoted by $B(l) = ((p_1,q_1),(p_2,q_2),\ldots,(p_i,q_i),(p_{i+1},q_{i+1}),\ldots,(p_n,q_n))$, where $L(p_i) = l$ and $L(q_i) \neq l$. Then, there is a node on the region boundary whenever $L(q_i) \neq L(q_{i+1})$, and the node position can be computed by the following equation (see [8]):

$$\eta_i = \frac{1}{2}\left(p_i + q_i + d_{p_i,q_i} + \begin{bmatrix} 1 \\ 1 \end{bmatrix} \right) \tag{2}$$

Further, an edge is represented as a quadruple:

$$E(\eta_i, \eta_j, l_l, l_r), \tag{3}$$

which records its two connected nodes and the labels of the two adjacent regions separated by this edge E. The nodes are shown as shaded circles in Figure 1(c), where the thick lines between two nodes are the edges of the weighted graph. The details for computing the edge weights can be found in [8]. Once the weighted graph is constructed, the remaining algorithm is the same as the pixel-based approach. However, when compared with the pixel-based approach, the number of graph nodes created by the region-based approach is much less, and hence the computational cost can be greatly reduced.

3. New Intelligent Scissors

The intelligent scissors described in the previous section is a good interactive tool for image segmentation. Our goal is to develop new techniques that can further reduce human efforts in manual operation. The major contribution of this paper is to achieve the above goal by incorporating the following two techniques into the intelligent scissors. The first technique is the multi-scale image segmentation that can prevent the user from being interfered by weak and irrelevant details. The second technique is the trail-dependent scheme that utilizes the information contained in the trail of the cursor's motion. The former will be introduced in Section 3.1 and the latter in Section 3.2.

3.1 Multi-Scale Intelligent Scissors

In Section 2, we have reviewed a region-based intelligent scissors, which constructs a weighted graph based on the image partition produced by the toboggan algorithm. The toboggan algorithm is in fact an algorithm for implementing watershed segmentation.

During the last decade, watershed segmentation has become a popular technique for different applications that require image segmentation, such as machine inspection, aerial image understanding, medical image analysis, and video object segmentation [1][3][4][8][10][12][13]. There are two approaches to implementing watershed segmentation: immersion simulation and toboggan simulation. Conceptually, the immersion simulation can be viewed as a "bottom-up" approach, and the toboggan simulation a "top-down" approach. It has been shown that both approaches can lead to the same segmentation results.

In watershed segmentation, one can imagine the watershed regions to be the catchment basins, and the region boundary to be the ridges around the basin. The desired object boundaries almost always occur at the boundaries of those watershed regions. Notice that a higher ridge implies stronger evidence that an object boundary exists. Based on the relative height of the ridge, some researchers [9][11] have proposed methods for constructing watershed regions with a hierarchical representation. To construct a hierarchical representation of segmentation, each boundary segment is assigned a value, called "dynamics", when constructing watershed regions [9]. The dynamics of a ridge is defined to be the minimal height from bottom of basin to the ridge. Given a dynamic threshold, T_{dyn}, connecting regions sharing a ridge having a dynamics smaller than the threshold will be merged. Therefore, by adjusting the dynamic threshold, T_{dyn}, one can determine the desired level of watershed segmentation in the hierarchical representation. If a segment of region boundary exists at a coarser level of the hierarchical representation, it implies that this segment of region boundary is more salient or more important in image segmentation. Figure 2(b) shows the dynamics of the region boundaries, where the darker lines represent the region boundaries having larger dynamics.

Usually, the desired object boundaries follow the segments of region boundary that have higher dynamics. When tracing the object boundary at a coarser level of the hierarchical segmentation, the human operator can move the cursor with less stress since it is less likely to be interfered by weaker or unimportant edge signals. Furthermore, the lengths of the boundary segments at the coarser level tend to be longer than those at the finer level.

Here, we describe a technique for integrating multi-scale image segmentation into the intelligent scissors. When constructing the weighted graph based on multi-scale watershed segmentation, we modify the edge representation described in Equation (3) as follows in order to include the dynamics of the graph edge:

$$E(\eta_i, \eta_j, l_l, l_r, d) \tag{5}$$

where *d* is the dynamics of the edge *E*. Before performing the shortest path search, we first determine whether an edge should be considered or not with a given dynamic threshold T_{dyn}. The edge will only be considered if its dynamics is larger than T_{dyn}. Notice that if the threshold T_{dyn} is set to be zero, the obtained optimal path will be exactly the same as that obtained by the conventional (finest level) region-based intelligent scissors. Figure 3 illustrates the different results obtained by applying the intelligent scissors at different levels of watershed image segmentation. In this experiment, we arbitrary select a seed node, marked as "$\oplus$", and then move the cursor to an image position, marked as "+" in the upper row of the images. The lower-row images show the watershed regions constructed with different dynamics thresholds, T_{dyn}, and the darkest line indicates the optimal path found between the seed point and the cursor point. Figure 3(a) shows the result obtained at the finest level, which is exactly the same as that obtained by the conventional region-based intelligent scissors, and Figures (b) and (c) show the result obtained at the middle and coarser levels, respectively. It can be seen that the manual operation at the coarser level can extract the desired object boundary without placing the cursor right at the desired region boundaries, which allows the human operator to manipulate the cursor with less tension.

3.2 Trail-Dependent Intelligent Scissors

When extracting object contours from a single image using an intelligent scissors, the user usually has to select a sequence of optimal path by carefully clicking some nodes along the object boundary. The information contained in the trail of the cursor's motion, which somewhat implies the intention of the human operator, is not used in the conventional intelligent scissors. In this section, we introduce a new trail-dependent intelligent scissors, which utilizes the information contained in the cursor's trail, and hence can allow the user to extract the desired object boundary with less mouse-clicking, and hence is more user-friendly.

First, we apply the same procedure as the conventional region-based intelligent scissors to create a weighted graph. Next, we record the cursor's trail while the human operator is moving the cursor to select the optimal path. In our implementation, we record the cursor's trail in an ROI (region of interests) map. The ROI map is of the same size as the input image. While the human operator is dragging the cursor in the input image, we mask the pixel in the ROI map corresponding to the cursor position to be a part of ROI. To allow the human operator to move the cursor more freely, we let the cursor have an effective area. We use a mask window centered at the current cursor point to record the cursor's trail in the ROI map. That is, we assume that all the pixels falling within the mask window are the region in which the human operator is interested. We called this mask window the cursor window, *W(p)* , corresponding to the cursor position *p*. When moving the cursor around, we may produce some discrete or discontinuous cursor points. Therefore, we may need to interpolate between the current cursor position and the last cursor position, and then recorded it the ROI map. To start with, the human operator first selects the first seed node. Once the human operator begins to move the cursor, the ROI map will be updated. Then, we perform the shortest path search algorithm as the conventional region-based approach, except that all shortest paths must lie within the ROI. This constrained search will be referred to as *the ROI shortest path search* from now on. This simple method works well in finding the desired optimal path from the seed node to the cursor node. However, it will fail when the ROI is connected to be a closed path along desired object contour. The desired path is the closed contour, but unfortunately the optimal (shortest) path from the seed node to the cursor node is not. To solve this problem, we must determine whether the cursor’s trail is a closed path or not. Hence, we need to know where is the head of the cursor’s trail and when the cursor’s trail begins to form a closed path. The former problem can be solved by selecting the first seed node to be the head of cursor’s trail. But the latter problem is more troublesome. It is possible that the cursor may leave from the first seed node and then begin to approach it again. But it is also possible that the human operator would like to select the optimal path around the first seed node. To distinguish between these two situations, we assume that the cursor’s trail will form a closed path only after the cursor has moved out of the bounding area of the first seed node and entry again. Centered at the first seed node, we define two areas, the core area and the bounding area, to help determining the cursor state. The cursor state is either the initial state, the starting sate, the developing state, the alerting, or the ending state. The bounding area is used to determine whether the cursor is moving out or is reentering. The core area is used to determine whether the process should be terminated or not. Figure 4(a) shows the relationship between the core area and the bounding area. The state diagram shown in Figure 4(b) illustrates the transition of the cursor state. The description of each event is listed in Table 1. At the very beginning, we initialize the cursor state to be the initial state. In the initial state, the only process is waiting for the human operator to select the first seed node, and then the cursor state is switched into the starting state. After entering the starting state, the state is checked whenever the human operator is moving the cursor. Further, the ROI map will be updated and the ROI shortest path search is performed to compute the optimal paths, until the cursor state is switched into the ending state.

Event Number	Description of the event
1	The human operator selects the first seed node
2	Cursor is moved inside the bounding area
3	Cursor is moved out of the bounding area
4	Cursor is moving outside of the bounding area
5	Cursor is moved into the bounding area
6	Cursor is moved out of the bounding area again
7	Cursor is moving inside the bounding area
8	Cursor is moved into the core area

Table 1: List of events.

In the starting state, the human operator can move the cursor around the first seed node but the cursor trail will never be considered as a closed path. When the cursor is moved out of the bounding area, the state is switched into the developing state. The developing state implies that the cursor has left the first seed node, and is allowed to enter the alerting state. When the cursor state is switched into the alerting state, it means the cursor’s tail is getting close to the first seed node and the trail is about to define a closed contour. To avoid losing the already found optimal path (referred to as the major path) from the seed node to the last cursor node before entering the bounding area, we set that last cursor node to be a new seed node automatically (i.e., without the user's clicking button). Further, we also backup the ROI map. If human operator does not like the new seed node, he/her can moves cursor out of the bounding area again. Then, we will delete the new seed node and rollback the previous ROI map. Once the cursor finally moves into the core area, the cursor state will be switched into the end state. We then update the ROI map and set the cursor node to be the new seed node. Next, we will perform the ROI shortest path search to compute two optimal paths, referred to as the minor paths. One is the optimal path between the last seed node and the current cursor node. The other is the optimal path from the cursor node to the first seed node. Finally, the desired object contour can be obtained by connecting the major path with the above two minor paths. Figure 5 compares the image segmentation results obtained by using the trail-dependent and trail-independent intelligent scissors. As shown in Figure 5(a), we first select node A to be the initial seed node, and then move the cursor to node B, C, D, E and F, successively. The object boundaries extracted by the trail-independent intelligent scissor at different stages are shown in Figures 5(a), 5(b), 5(c), 5(d), 5(e) and 5(h). On the other hand, the object boundaries extracted by our trail-dependent intelligent scissors are shown in Figures 5(a), 5(b), 5(c), 5(d), 5(g) and 5(j). When the cursor is moved from A to B, to C and to D, the results obtained by both methods are the same. However, if the cursor continues to move to E and then to F, the trail-dependent method can still extract the desired object boundary, while the trail-independent one will favor an undesired shorter path. Notice that Figures 6(f) and 6(i) show the cursor's trail and ROI map corresponding to Figures 6(g) and 6(j). Here, the cursor position is indicated by darker dots, which falls within the shaded region representing the ROI.

4. Some Experimental Results

Some experimental results are shown in this section in order to illustrate the advantages of the new intelligent scissors proposed in this paper. All of the seed nodes (i.e., the graph nodes selected by clicking the mouse button) are indicated by the symbol "⊕" and the current cursor point is indicated by the symbol "+" in those figures that show the extracted object boundary. However, for those figures that show the cursor's trail, the seed nodes are indicated by the symbol "+" and the successive cursor positions that constitute the cursor's trail are indicated by black dots.

First, consider Figure 6. Figure 6(a) shows the source image, and Figure 6(b) shows the watershed regions constructed with a relatively large dynamics threshold. To begin with, we arbitrarily click a seed node residing on the desired object contour, and then move the cursor to extract the desire object boundary. When the cursor is moving, the ROI map will be updated and then the shortest path search in ROI will be performed to compute the optimal path for each node within the ROI. Figures 6(c) and 6(e) show some intermediate results of the optimal path from the seed node to the cursor node. After the cursor is moved out of the bounding area (defined in Section 3.2), if it is moved into the bounding area again, our algorithm will select a new seed node automatically. Figure 6(g) shows two seed nodes, one is the initial seed node selected manually and the other is the one selected automatically by our algorithm. Finally, the extracted object boundary is the white line shown in Figure 6(g). With our trail-dependent intelligent scissors, object extraction for simple images, such as the one shown in Figure 6, usually requires only one initial button clicking, followed by simple casual tracing.

The next example is more complex than the first one. Figure 8(a) shows the source image used in the second example. Before tracing the object boundary, the user can first select a dynamics threshold (if he does not like the default one) so that most of the desired boundaries can appear at this level of watershed segmentation. For example, the watershed regions obtained with a relatively high threshold is shown in Figure 8(b).

First, we select an initial seed node, as shown in Figure 7(c), and then move the cursor along the desired object boundary. When the cursor is moving around, the extracted boundary corresponding to the moving cursor will be displayed on-line to provide interactivity. However, as the cursor moves to the image position marked by "+", as shown in Figure 8(e), the extracted boundary did not continue to grow as one might expect. This is because we have selected a relatively high dynamics threshold, and thus the desired boundary segment did not appear in the result of watershed segmentation. The cursor trail and the ROI map at this moment can be found in Figure 7(f).

One solution is to lower down the dynamic threshold to allow the weaker boundary appeared in the watershed segmentation results. After decreasing the dynamics threshold, the watershed regions obtained are shown in Figure 8(b). It can be seen that the watersheds shown in Figure 8(b) contain more details than those shown in Figure 7(b), and hence, the desired boundary missing in Figure 7(e) can be extracted in Figure 8(a). Similar situation occurs in Figures 8(c) and 8(e). In Figure 8(e) the dynamics threshold is set to 0 and almost all the details are included. However, more caution has to be taken and more careful clicking has to be performed by the user. For example, two extra seed nodes are selected in Figure 8(e). One is for reserving previous optimal path before lowering down the threshold, and the other is for avoiding the interference from other details. After extracting the desired weak boundary, we can increase the dynamics threshold to lessen the stress caused by the requirement of accurate (or high-resolution) cursor movement and mouse clicking. This can be seen in Figures 8(g) and Figure 8(h). Repeating the above procedure, we can extract the desired object contour as shown in Figure 9(a). The trail of the cursor is recorded in Figure 9(b).

Based on the multi-scale scheme, the human operator can decrease the dynamics threshold to select the detailed edge of desired object boundary. Nevertheless, it is possible that certain segment of the desired object boundary turns out to be not portion of any optimal paths, even it is an edge of the weighted graph. To solve this problem, our tool includes two other operation modes. One is the edge-selection mode and the pixel-selection mode. In the edge-selection mode, when human operator clicks a node, all the edges connecting to this node will be displayed, and then the user can select desired edge. If the desired boundary segment is not even an edge of the weighted graph associated with the finest watersheds, we can turn to the last resort, which is the pixel-selection mode, where the human operator can zoom in the image and select the desired boundary point pixel by pixel.

5. Conclusions

In this paper, we have presented a new interactive image segmentation tool, which combines two techniques, the trail-dependent scheme and the multi-scale image segmentation, with the region-based intelligent scissors. This new method for interactive image segmentation has two major advantages over the conventional intelligent scissors. The first one is due to the utilization of the cursor trail, which contains the information related to the intention of the human operator. The use of the trail information makes our trail-dependent intelligent scissors require less mouse-clicking, and hence is more user-friendly. The second advantage is due to the use of multi-scale watershed segmentation, which prevents the user from being interfered by weak and irrelevant details and allows the user to trace the object boundary with less tension. Another power of using multi-scale watershed segmentation is that it allows the user to easily adjust the coarseness of segmentation and adaptive to different image content. Our experiments have demonstrated that this new interactive segmentation tool is highly flexible for any situation, and in general requires less human efforts than the previously available tools.

References

1. M. Couprie and G. Bertrand, "Topological Grayscale Watershed Transformation", *SPIE Vision Geometry V Proceedings*, Vol. 3168, 136-146, 1997.
2. D. Geiger, A. Gupta, L.A. Costa, and J. Vlontzos, “Dynamic Programming for Detecting, Tracking, and Matching Deformable Contours,” *IEEE Trans. Pattern Analysis and Machine Intelligence*, **17**(3), pp. 294-302, 1995.
3. Srinka Ghosh e t al., “Watershed Segmentation of High Resolution Magnetic Resonance Images of Articular Cartilage of the Knee”, *IEEE Proc. Conf. EMBS*, Vol. 4, pp. 3174-3176, 2000.
4. Michael W. Hansen and William E. Higgins, “Watershed-Based

Maximum-Homogeneity Filtering”, *IEEE Trans. Image Processing*, **8**(7), pp. 982-988, 1999.

5. M. Kass, A. Witkin, and D. Terzopoulos, “Snakes: Active Contour Models,” *Int. Journal of Computer Vision*, **1**(4): 321-331, 1988.
6. E. N. Mortensen and W. A. Barrett, "Intelligent Scissors for Image Composition," in *Computer Graphics (SIGGRAPH `95)*, pp. 191-198, 1995.
7. E. N. Mortensen and W. A. Barrett, "Interactive Segmentation with Intelligent Scissors," *Graphical Models and Image Processing*, **60**(5), pp. 349-384, 1998.
8. E. N. Mortensen and W. A. Barrett, "Toboggan-Based Intelligent Scissors with a Four Parameter Edge Model," in *Proc. IEEE: Computer Vision and Pattern Recognition (CVPR'99)*, Vol. II, pp. 452-458, June 1999.
9. L. Najman and M. Schmitt, “Geodesic Saliency of Watershed Contours and Hierarchical Segmentation,” *IEEE Trans. Pattern Analysis and Machine Intelligence*, **18**(12), pp. 1163-1173, 1996.
10. C. Riddell et al., “TheWatershed Algorithm: A Method to Segment Noisy PET Transmission Images”, *IEEE Trans. Nuclear Science*, **46**(3,2), pp. 713-719, 1999.
11. L. Vincent, “Morphological Grayscale Reconstruction in Image Analysis: Applications and Efficient Algorithms,” *IEEE Trans. Pattern Analysis and Machine Intelligence*, **2**(2), pp.176-201, 1993.
12. L. Vincent and P. Soille, “Watersheds in Digital Spaces: An Efficient Algorithm Based on Immersion Simulations,” *IEEE Trans. Pattern Analysis and Machine Intelligence*, **13**(6), pp. 583–598, 1991.
13. D. Wang, “Unsupervised Video Segmentation Based on Watersheds and Temporal Tracking,” *IEEE Trans. on Circuits and Systems for Video Technology*, **8**(5), pp. 539–546, 1998.
14. D.J. Williams and M. Shah, “A Fast Algorithm for Active Contours and Curvature Estimation,” *CVGIP: Image Understanding*, **55**(1), pp. 14-26, 1992.

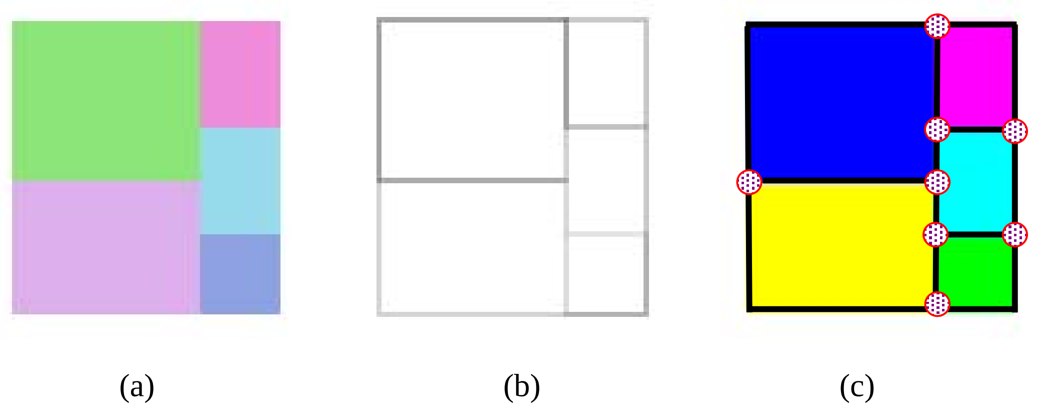

Figure 1: An example of watershed segmentation: (a) source image, (b) gradient image, (c) result obtained by watershed segmentation. Different regions are labeled with different colors. The shaded circles indicate the nodes of the weighted graph used for finding the optimal path.

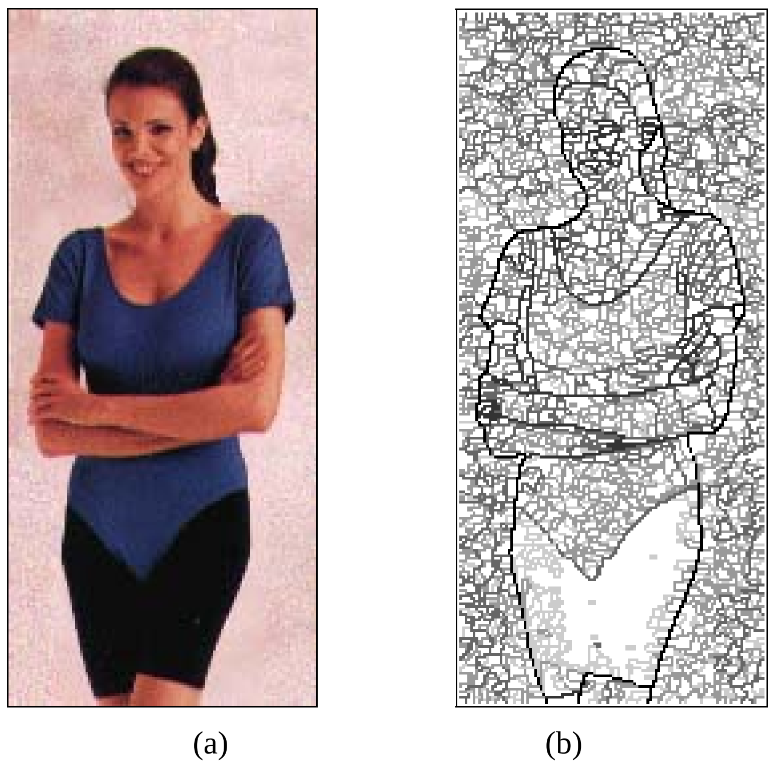

Figure 2: An example of the hierarchical representation of watershed. (a) Source image. (b) Watershed regions. The region boundary segments marked by darker lines have higher dynamics.

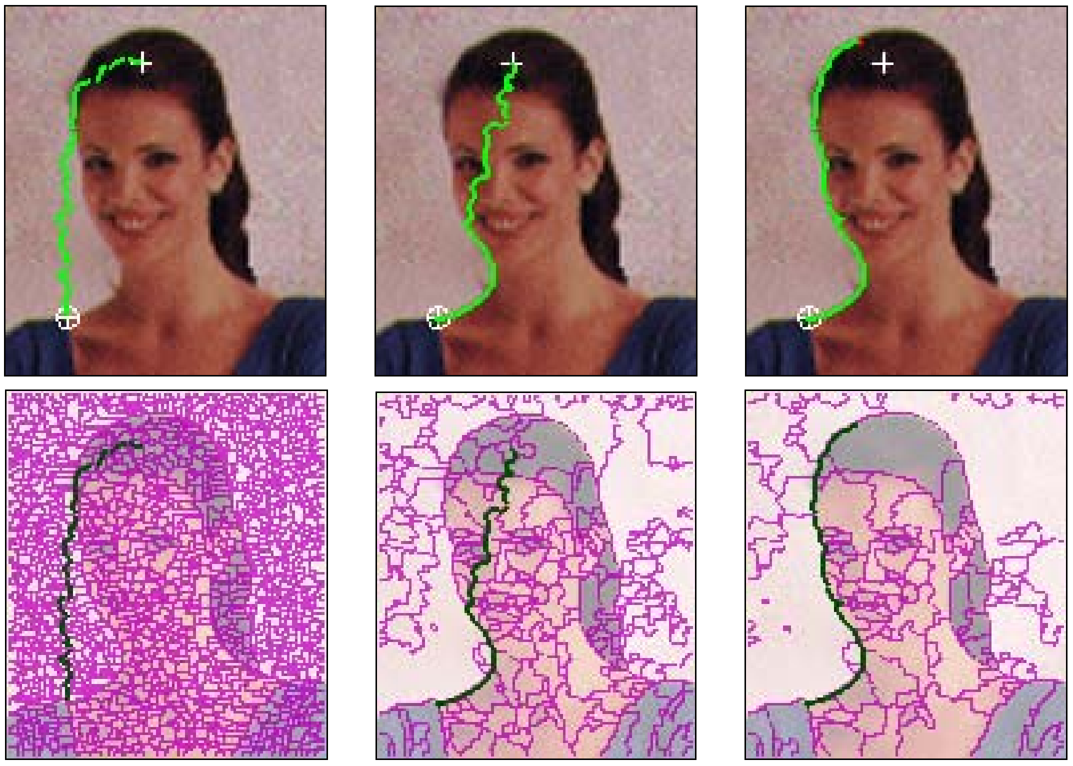

Figure 3: An example of multi-scale intelligent scissors with (a) smallest (b) middle and (c) largest T_{dyn}. The images on the upper row shows the extracted boundary from the seed point, $\oplus$, to the cursor node that is nearest to the current cursor point, +. The images on the lower row show the watershed regions and the optimal paths at different levels.

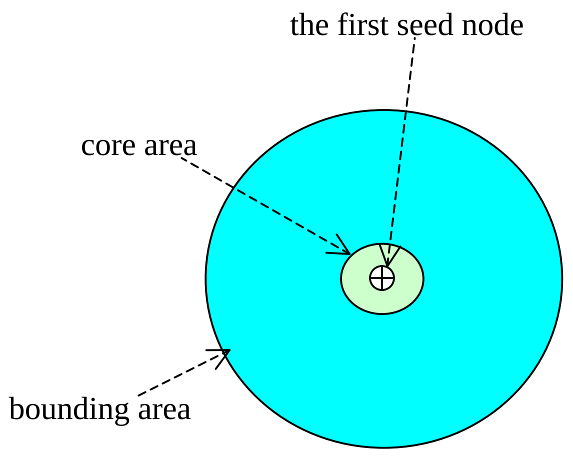

(a)

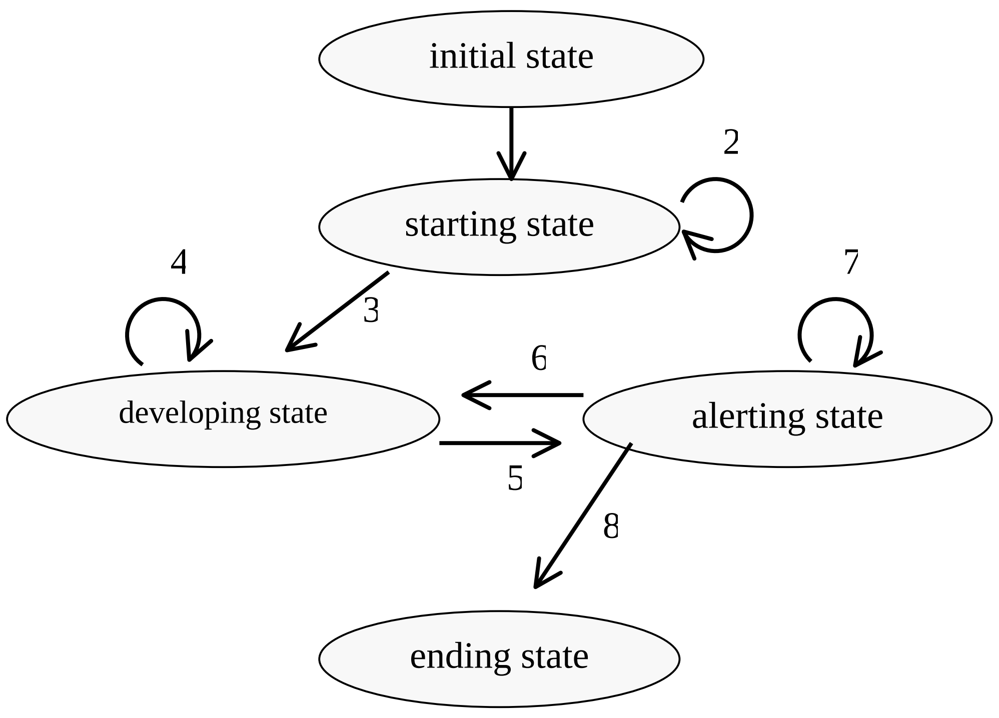

(b)

Figure 4: The state diagram for determining the cursor state. (a) shows the relationship between the core area and the bounding area. (b) shows the state diagram. The elliptical circles are the states. The state transitions are shown by using arrows with a number indicating the associated event. Descriptions of the corresponding event are summarized in Table 1.

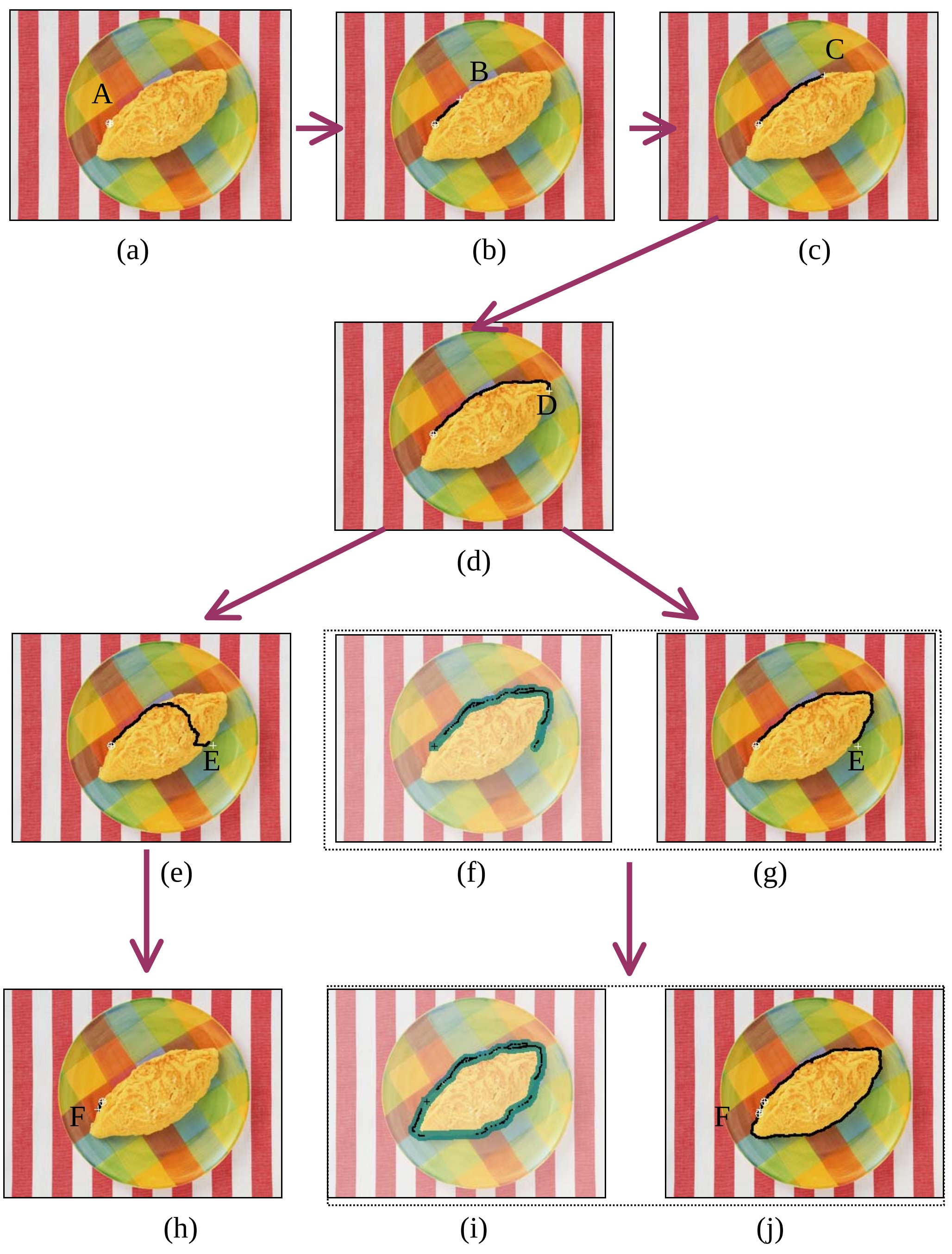

Figure 5: Comparison between trail-independent and trail-dependent intelligent scissors. (a),(b),(c),(d),(e), and (h) show the results of image segmentation obtained by using the trail-independent intelligent scissors. (a),(b),(c),(d),(g),(j) show the results obtained by using the trail-dependent intelligent scissors. The darker strokes in (f) and (i) are the cursor's trails of (g) and (j), respectively. The black dots are the cursor position.

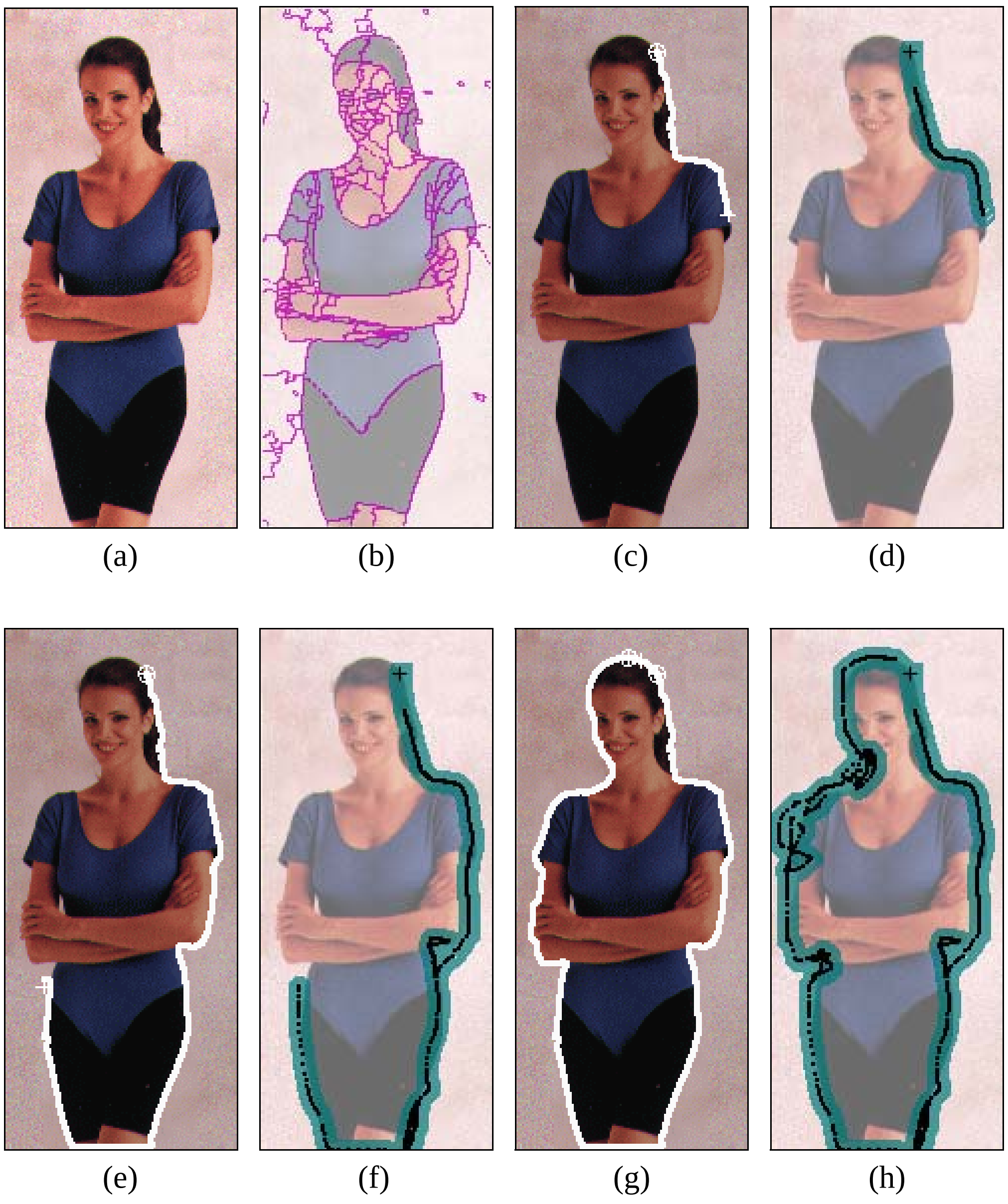

Figure 6: An example of image segmentation using the trail-dependent and multi-scale scheme. (a) shows the source image, and (b) shows the watershed regions obtained with a high dynamics threshold. (c) and (e) are intermediate results, and the corresponding cursor trail is shown in (d) and (f), respectively. (g) shows the segmentation result and (h) shows its cursor trail.

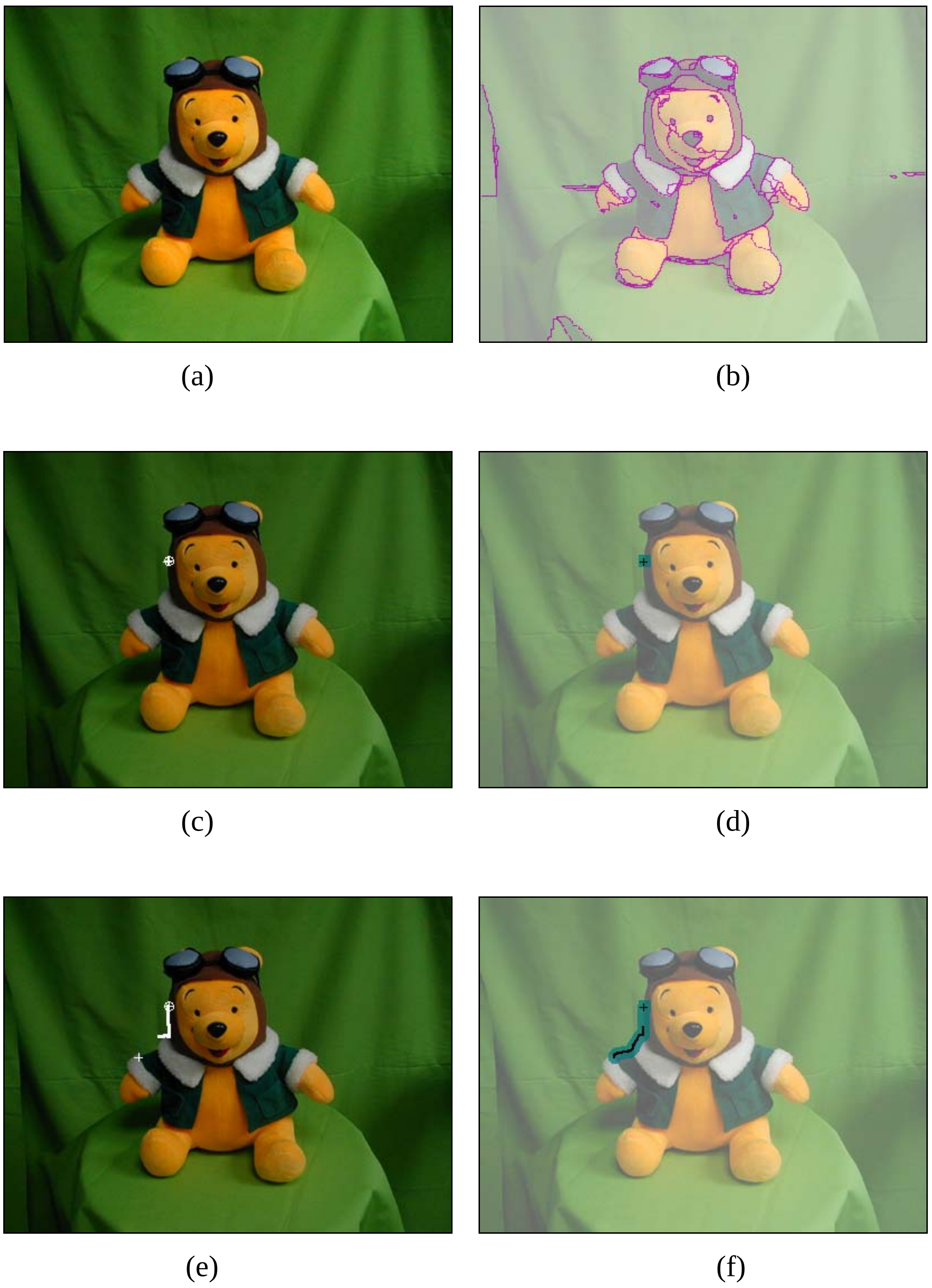

Figure 7: An example of image segmentation using the trail-dependent intelligent scissors based on multi-scale watershed image segmentation. (a) Source image. (b) Watershed regions with a relatively high dynamics threshold. (c) and (e) are the intermediate results, and (d) and (f) show the corresponding cursor trail. In (e), the seed node is marked by $\oplus$ and the current cursor by "+". There exists no watershed ridge (with the chosen dynamics threshold) on the desired object boundary. Hence, the desired object boundary can not be extracted.

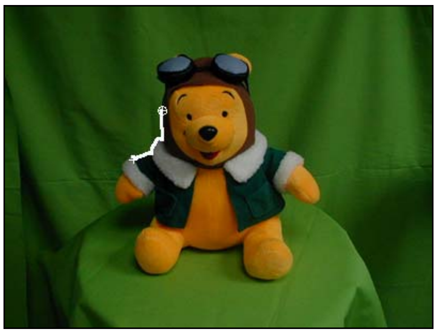
(a)

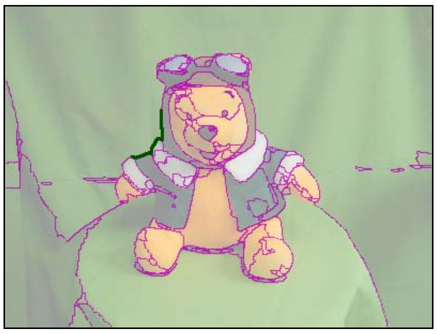
(b)

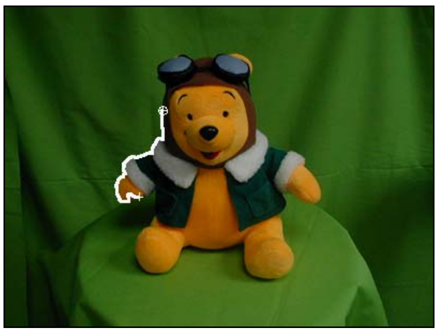
(c)

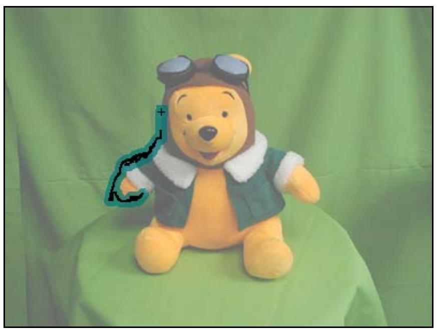
(d)

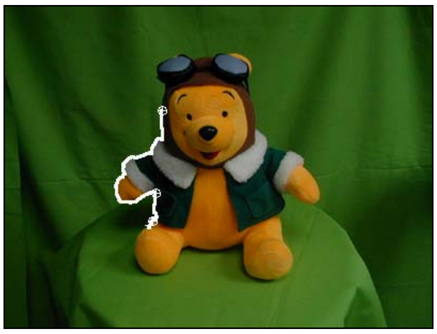
(e)

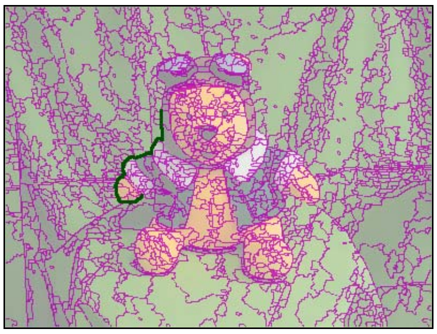
(f)

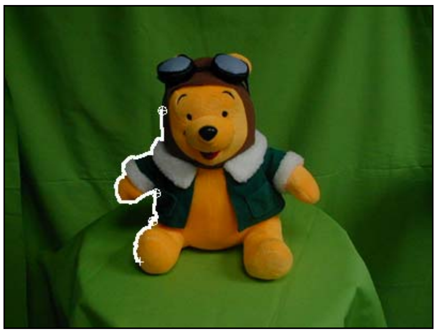
(g)

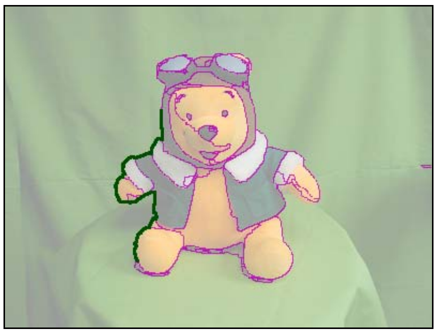
(h)

Figure 8: The continued example of Figure 7. In Figure 7, the initial dynamics threshold used is too high to reserve weak object boundaries. Here, we lower down the dynamics threshold such that the desired weaker boundaries can also appear, as shown in (a), (c) and (e). (b), (d), (f), and (h) are the watershed regions corresponding to (a), (c), (e) and (g), respectively. Notice that in (h) we raise up the dynamics threshold in order to reduce the interference caused by weak edges.

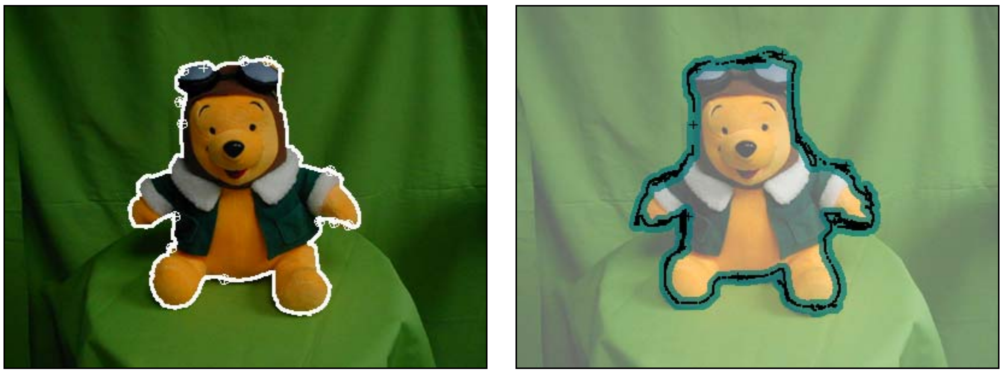

(a) (b)

Figure 9: The final results of image segmentation. (a) the extracted object boundary and (b) the trail of the cursor.